Chemical Engineering Journal 165 (2010) 751–757

Contents lists available at ScienceDirect

Chemical Engineering Journal

journal homepage: www.elsevier.com/locate/cej

Efficient removal of Cu(II), Pb(II), Cr(VI) and As(V) from aqueous solution using an aminated resin prepared by surface-initiated atom transfer radical polymerization

Li Niu, Shubo Deng*, Gang Yu, Jun Huang

Department of Environmental Science and Engineering, POPs Research Center, Tsinghua University, Beijing 100084, China

ARTICLE INFO

Article history:
Received 19 June 2010
Received in revised form 15 August 2010
Accepted 22 August 2010

Keywords:
ATRP
Aminated resin
Heavy metal removal
Sorption capacity
Sorption mechanism

ABSTRACT

A novel aminated resin for the efficient removal of Cu(II), Pb(II), Cr(VI) and As(V) ions from aqueous solution was prepared via surface-initiated atom transfer radical polymerization (SI-ATRP) and subsequent amination reaction. Polyglycidyl methacrylate (PGMA) was first grafted from the merrifield chloromethylated resin (MCR) via SI-ATRP of GMA, and then ethylenediamine was used for amination to produce the aminated resin. Fourier transform infrared (FTIR) and X-ray photoelectron spectroscopy (XPS) as well as scanning electron microscopy (SEM) were used to characterize the grafted PGMA brushes and amine groups on the functionalized MCR surfaces. XPS spectra and sorption behaviors confirmed that the amine groups were responsible for efficient Cu(II) and Pb(II) removal via chelation, while the electrostatic interaction between the protonated amine groups and anionic species dominated the sorption of Cr(VI) and As(V). The sorption equilibrium of As(V) was achieved within 1 h, much faster than others. According to the Langmuir fitting, the maximum sorption capacities of Cu(II), Pb(II), Cr(VI) and As(V) on the aminated resin at pH 5 were 2.6, 0.97, 3.0, and 2.2 mmol/g, respectively. SI-ATRP technology is an effective approach to prepare adsorbents with high sorption capacity for some pollutants.

1. Introduction

Adsorption is one of the methods commonly used in wastewater treatment. Surface functional groups of adsorbents not only affect the sorption behavior, but also dominate the sorption mechanism. Adsorbents with carboxyl, sulfonic and phosphonic groups on the surface remove adsorbates through ion exchange, while those containing nitrogen such as amine, hydrazine, thioamide, and imidazoline groups not only chelate cationic metal ions, but also adsorb anionic adsorbates through electrostatic interaction [1–3]. In particular, amine groups have been found to belong to the most effective groups for pollutant removal from aqueous solutions [2,4–7].

Sorption capacity is one of the important characteristics in the evaluation of adsorbents, and the increase of the density of functional groups on sorbent surfaces may increase the sorption capacity. Some low molecular weight chemicals are often used to modify the material surface [2,8], but the enhanced adsorption capacity is not very satisfactory due to the limited adsorption sites on the matrix materials. To increase the density of functional groups, macromolecules were loaded physically onto the materials [9,10], but such macromolecules are easy to break off from the matrix materials as no chemical bonds exist between them. Polymerization reaction offers potential applications in surface modification where polymer chains can be attached covalently onto the material surface, making polymers wrap on the solid surface firmly [11].

Surface-initiated atom transfer radical polymerization (SI-ATRP) has been extensively investigated for grafting polymers from surfaces in a controlled manner in recent years [12,13], SI-ATRP can be performed with various functional monomers and owns simple synthetic routes [14]. Although SI-ATRP has been utilized extensively for the preparation of active polymer brushes on functional materials [15,16], few studies reported the utilization of ATRP for adsorbent modification [17–20]. Li et al. reported that grafted polyacrylamide from chitosan beads via ATRP can enhance the sorption capacity for mercury ions [18]. Li et al. also reported that the poly(hydroethyl acrylate)-grafted cross-linked poly(vinyl chloride) particles via ATRP can selectively remove Cu(II), Hg(II), Zn(II), and Cd(II) ions from water [18]. Senkal and Yavuz modified the poly(styrene-divinyl benzene) resin using ATRP for the removal of dyes from water [19].

Earlier studies have indicated that benzyl chloride is an effective initiator for surface-initiated ATRP from a variety of substrates [17,20]. Merrifield chloromethylated resin (MRC) itself contains many benzyl chloride initiation sites and was used in this study.

* Corresponding author. Tel.: +86 10 62792165; fax: +86 10 62794006.
E-mail address: dengshubo@tsinghua.edu.cn (S. Deng).

1385-8947/$ – see front matter © 2010 Elsevier B.V. All rights reserved.
doi:10.1016/j.cej.2010.08.053

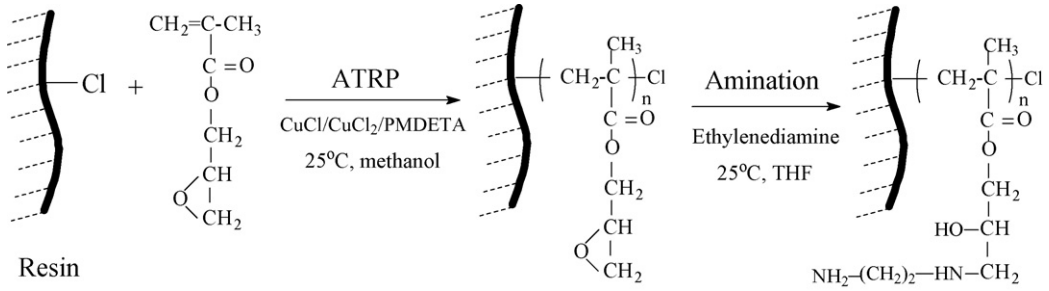

Scheme 1. Schematic diagram illustrating the preparation process of the aminated resin by the combined SI-ATRP and amination reactions.

PGMA was first grafted from the MRC via SI-ATRP, and then the aminated MRC was prepared through ring-opening reaction of PGMA brushes with ethylendiamine (see Scheme 1). The aminated resin was used to efficiently remove Cu(II), Pb(II), Cr(VI) and As(V) ions from aqueous solution. Batch sorption experiments were conducted to investigate their sorption behaviors including sorption kinetics, isotherm, and effect of solution pH. The adsorbent was characterized by SEM, FTIR and XPS, and the sorption mechanism was also discussed according to the sorption behaviors and XPS spectra.

2. Materials and methods

2.1. Materials

Merrifield chloromethylated resin (MCR, 2.5–4.0 mmol Cl/g, 1% cross-linked), glycidyl methacrylate (GMA, >97%), ethylendiamine and N,N,N,N,N-pentamethyldiethylenetriamine (PMDETA, 99%) were purchased from Aldrich Chemical Co. of Milwaukee. GMA was passed through a silica gel column to remove the inhibitor, and stored under an argon atmosphere at −10 °C. Copper(I) chloride (CuCl, 99%) and copper(II) chloride ($CuCl_2$, >97%) were obtained from Sinopharm Chemical Reagent Co., Ltd. Other chemicals are used as received.

2.2. Preparation of aminated resin via SI-ATRP

Graft polymerization of GMA from the MCR (MCR-*g*-PGMA) was achieved through the benzyl chloride initiation sites on the MCR. A typical procedure is as follows: MCR (1.0 g) was transferred into a tube with the mixture of ultrapure water (1 mL), methanol (2 mL), GMA (3 mL) and PMDETA (120 μL). The reaction solution was purged with nitrogen for about 20 min and then CuCl (60 mg) and $CuCl_2$ (12 mg) were added into the tube. The tube was then sealed and shaken in an orbital shaker at 150 rpm and 25 °C for a predetermined time from 10 to 115 min. The obtained MCR-*g*-PGMA was filtered and washed thoroughly with tetrahydrofuran (THF) to ensure the complete removal of the physically adsorbed reactants.

In the ring-opening (amination) reaction, the dried MCR-*g*-PGMA (about 1.0 g) was put into the tube containing 2 mL of THF and 4 mL of ethylenediamine. The reaction mixture was shaken at 150 rpm and 25 °C for different time. After the reaction, the aminated resin was washed thoroughly with acetone and deionized water sequentially. Finally, 0.1 M HCl was used to remove the copper residue completely, and then 0.1 M NaOH solution was used to neutralize the excess acid. After being rinsed with deionized water till neutral, the aminated resin was dried at room temperature until constant weight.

During the optimization of adsorbent preparation, the following sorption experiments were carried out to evaluate the sorption capacity. The sorption experiments were conducted in 250 mL flasks, each of which contained 100 mL of 2 mmol/L $CuSO_4$ solution at pH 5. After 50 mg of adsorbent was added into each flask, the flasks were shaken in a shaker at 150 rpm and 25 °C for 24 h.

2.3. Adsorbent characterization

The adsorbents were characterized by SEM, FTIR and XPS. For FTIR analysis, the samples of MCR, MCR-*g*-PGMA, and aminated resin were dried at room temperature until constant weight. Their FTIR spectra were recorded on a Fourier transform infrared spectrometer (Perkin-Elmer 2000, USA) in the wavenumber range of 650–4000 cm^{-1} under ambient conditions. An attenuated total reflection (ATR) accessory was employed for all IR spectral acquisitions. For SEM observation, the surface morphologies of the pristine resin and the modified resin after ATRP and amination reactions were characterized using an environmental scanning electron microscope (ESEM, FEI Quanta 200 FEG). The samples of MCR, MCR-*g*-PGMA and aminated resin before and after the adsorption experiments at pH 5 were analyzed by XPS. XPS measurements were performed on an AEM PHI 5300X spectrometer with a monochromatized Al Kα X-ray source. The X-ray source was run at a reduced power of 150 W, and the pressure in the analysis chamber was maintained at less than 10^{-8} Torr during each measurement. All binding energies were referenced to the neutral C 1s peak at 284.8 eV to compensate for the surface charging effects. The software package XPS peak 4.1 was used to fit the XPS spectra peaks, and the full width at half-maximum was maintained constant for all components in a particular spectrum.

2.4. Batch sorption experiments

Batch sorption experiments were conducted to examine the sorption kinetics, isotherm, and the effect of solution pH. The sorption experiments were conducted in 250 mL flasks, each of which contained 100 mL of solution prepared with $CuSO_4{\cdot}5H_2O$, $Pb(NO_3)_2$, $K_2Cr_2O_7$ or $Na_2HAsO_4{\cdot}12H_2O$. 50 mg of adsorbent was added into each flask, and then the flasks were shaken in a shaker at 25 °C and 150 rpm for the predetermined time.

In the kinetic experiments, the initial concentrations of Cu(II), Pb(II), Cr(VI) or As(V) were 2 mmol/L, and the initial solution pH was adjusted to 5 (no pH adjustment in the sorption process). The sorption isotherm experiments were conducted at a constant pH value of 5, with initial adsorbate concentration varied from 0.4 to 2.5 mmol/L. In the pH effect experiments, the initial solution pH values were in the range of 2–5.5 for Cu(II) and Pb(II), and 3–10 for Cr(VI) and As(V), and the solution pH values were kept constant throughout the experiments. The initial adsorbate concentrations were 2 mmol/L. In case of pH control during the sorption process, NaOH or HCl solution was added at regular time intervals.

After adsorption, the adsorbent was separated from the solution by filtration through a 0.22 μm membrane, and the residual Cu(II),

Pb(II), Cr(VI) or As(V) concentrations in the filtrate were analyzed with an inductively coupled plasma optical emission spectrometry (ICP-OES, IRIS Interpid II XSP). The adsorption capacity was calculated according to the difference of adsorbate concentrations before and after adsorption. At the same time, the adsorbate-sorbed adsorbent separated from the solution was rinsed with ultrapure water, and then dried at room temperature for XPS analysis.

3. Results and discussion

3.1. Adsorbent preparation

The preparation process of the aminated resin is shown in Scheme 1. The amount of grafted PGMA on the resin after the ARTP reaction was studied. The grafting density is defined as GD (%) = $(W_a - W_b)/W_b$, where W_a and W_b represent the weights of the dry resin after and before grafting, respectively. As shown in Fig. 1a, the grafting density increased linearly with increasing ATRP time within 115 min, indicating an approximately linear increase in thickness of the grafted PGMA layer with polymerization time [16]. The monomer (GMA) concentration decreased substantially with increasing reaction time. The initially rapid rate of surface-initiated ATRP bacame diffusion-controlled. Chain termination on the surface, followed by bimolecular coupling or disproportionation reactions that consume the active chains, may also become important with increasing ATRP time [21,22]. Fig. 1a also presents the sorption capacity of Cu(II) on the aminated resin prepared at different ATRP time. It can be seen that the adsorption capacity increased linearly with increasing ATRP time within 75 min, which is positively correlated with the amount of the grafted PGMA on the resin. After 75 min, the increase of sorption capacity slowed down, which is possibly related to the pore blockage by the excess grafted polymer. Since the MCR used in the experiments is a gel-type resin, it will swell in methanol solution and the enlarged intraparticle pores are available for the graft reaction. With the increase of ATRP reaction time, longer PGMA brush formed on the internal and external surface in the resin. Since the pore volume is limited, the ATRP reaction has to cease when the pores are packed with polymers. According to the sorption capacity obtained in Fig. 1a, the ATRP time was maintained at 100 min in the following experiments.

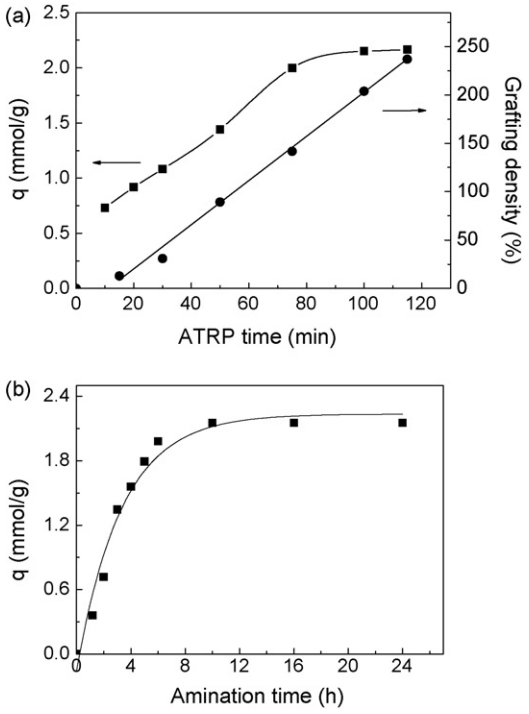

Fig. 1. Effects of (a) ATRP time on the sorption capacity of Cu(II) and grafting density and (b) amination time on the sorption capacity of Cu(II) on the aminated resin.

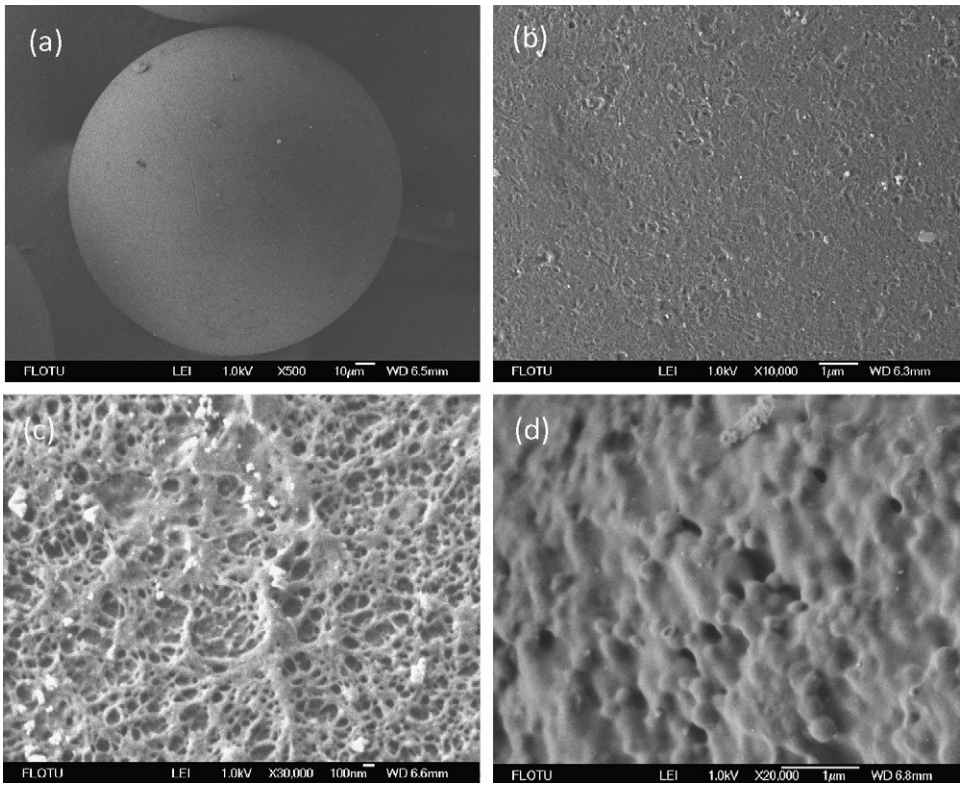

Fig. 2. SEM images of the resin before and after modification. (a) MCR (×500); (b) MCR (×10,000); (c) MCR-*g*-PGMA (×30,000); and (d) aminated resin (×20,000).

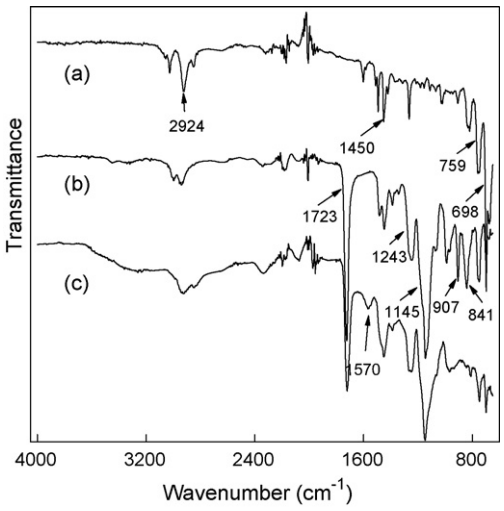

Fig. 3. ATR-FTIR spectra of the (a) MCR, (b) MCR-*g*-PGMA, and (c) aminated resin.

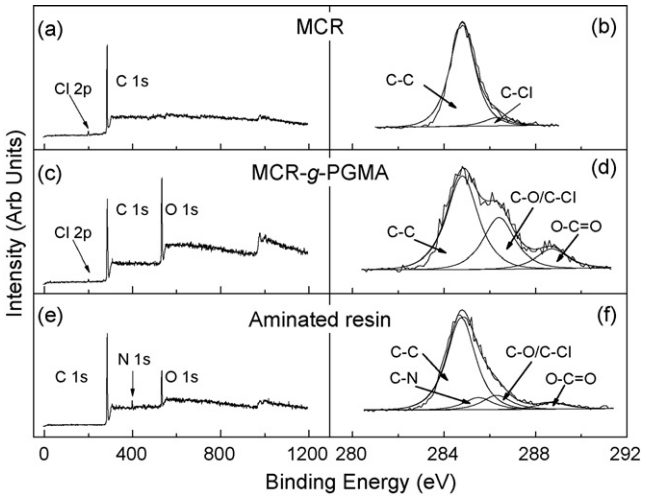

Fig. 4. XPS wide scan and C 1s core-level spectra of the MCR, MCR-*g*-PGMA, and aminated resin.

Fig. 1b illustrates the sorption capacity of Cu(II) on the aminated resin prepared at different ring-opening time. The adsorption capacity increased quickly within initial 6 h, and the equilibrium was achieved at around 10 h. Since the introduced amine groups were responsible for copper adsorption, the increasing sorption capacity indicated that more ethylenediamine molecules reacted with the epoxy groups in the grafted PGMA. This point will be verified in the following section. The ring-opening reaction was fixed at 12 h to prepare the aminated resin used in the following sorption experiments.

3.2. Adsorbent characterization

The morphologies of the resin before and after ATRP modification and amination reaction were observed using SEM. As shown in Fig. 2a and b, the surface of the pristine resin was relatively smooth. After the modification at ATRP time of 100 min, some net-like polymers were clearly observed on the PGMA-grafted resin surface (see Fig. 2c), indicating that the dense PGMA brushes were successfully grafted on the resin. Due to no steric hindrance, long PGMA brushes formed on the surface, while short PGMA chains may occur within the resin. Fig. 2d illustrates the morphology of the aminated resin after the ring-opening reaction, completely different from the resin surface after ATRP (Fig. 2c). The aminated resin surface became more hydrophilic after amino groups were introduced on the surface, possibly resulting in the change of surface morphology.

To identify the reactions, the FTIR spectra of the resin before and after modification were analyzed. Fig. 3 shows the ATR-FTIR spectra of the MCR, MCR-*g*-PGMA, and aminated resin. For MCR, the characteristic peaks at 2924 and 1450 cm^{-1} can be assigned to $-CH_2-$ stretching and skeleton vibration of the aromatic ring, respectively [23]. The peaks at 759 and 698 cm^{-1} are due to C–Cl stretching in $-CH_2Cl$ group [24]. After the resin surface modification, the typical peaks in the spectra in Fig. 3b and c changed significantly comparing with those in Fig. 3a. The graft of PGMA was confirmed by the appearance of strong peak at 1723 cm^{-1} (C=O stretching vibration in GMA) and two peaks at 1243 and 1145 cm^{-1} (C·O symmetric and asymmetric vibrations in GMA) [18,23]. The peaks at 907 and 841 cm^{-1} in Fig. 3b are the characteristic peaks of epoxy group, indicating the successful graft of PGMA on the resin [23]. These two peaks disappeared almost completely in Fig. 3c after the ring-opening reaction of epoxy groups with ethylenediamine. After the amination reaction, a broadband ranging from 3100 to 3700 cm^{-1} appeared. This wide band usually corresponds to the combination of the stretching vibration bands of both OH and NH groups [25], suggesting that –OH and –NH groups were introduced on the aminated resin surface. The –OH group arose from the ring-opening reaction of epoxy group with amine group (see Scheme 1). In addition, the new peak at 1570 cm^{-1} in Fig. 3c can be assigned to the deformation vibration of –NH groups, which further confirmed the introduction of amine groups on the resin surface [24].

XPS analysis was also used to analyze the change in the composition and functional groups of the resin surface after the ATRP and amination reactions. Fig. 4 illustrates the respective XPS wide scan and C 1s core-level spectra of the MCR, MCR-*g*-PGMA, and aminated resin. In Fig. 4a, the peak at about 200 eV attributed to Cl 2p is clearly visible, which suggests the existence of ATRP initiators on MCR surfaces. The C 1s core-level spectrum of MCR can be curve fitted with two peak components having binding energies (BEs) at 284.8 and 286.3 eV, corresponding to C–C and C–Cl species, respectively [26]. In comparison with Fig. 4a, the O 1s peak at about 532 eV emerged in both Fig. 4c and e, which is consistent with the successful graft of PGMA on the MCR surface. The C 1s core-level spectrum of MCR-*g*-PGMA in Fig. 4d can be curve fitted with three peak components with BEs of 284.8, 286.4, and 288.7 eV, attributable to the C–C, C–Cl/C–O, and O–C=O species, respectively [26]. This result indicates that PGMA was successfully grafted on the resin surface. After the ring-opening reaction, the N 1s peak at about 399 eV is observed in Fig. 4e, indicating that the amine groups were introduced on the resin surface. The corresponding C 1s core-level spectrum in Fig. 4f can be divided into four peak components with BEs of about 284.8, 285.5, 286.4 and 288.7 eV, attributable to the C–C, C–N, C–Cl/C–O and O–C=O species, respectively [26]. The XPS results are consistent with the FTIR results shown in Fig. 3.

3.3. Sorption kinetics

The aminated resin obtained via the ATRP and subsequent amination reactions was used to remove Cu(II), Pb(II), Cr(VI), and As(V) from aqueous solution. Fig. 5 shows their adsorption kinetics on the aminated resin. The sorption of As(V) on the aminated resin is the fastest among the four adsorbates. The sorption time for reaching equilibrium was 1 h for As(V), 6 h for Pb(II), 11 h for Cr(VI), and 20 h for Cu(II). Although all the initial concentrations of the four adsorbates were 2 mmol/L, their sorption capacities at the equilibrium time were different. The sorption capacity of Cu(II) was high up to

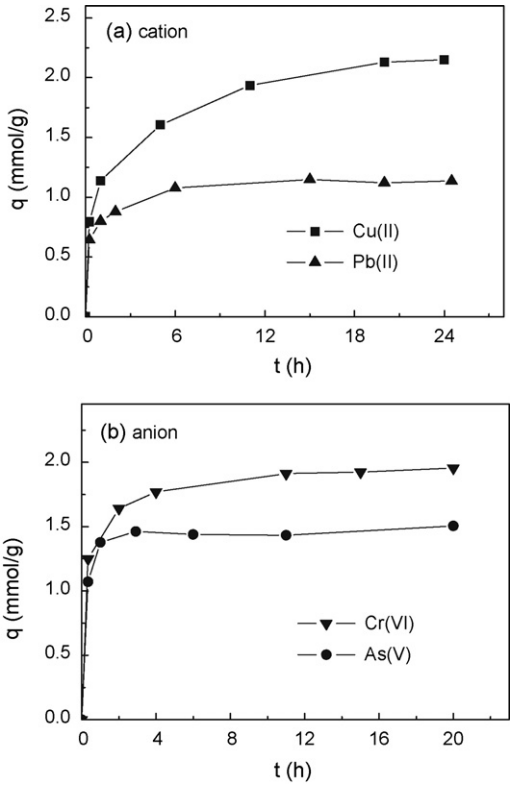

Fig. 5. Sorption kinetics of Cu(II), Pb(II), Cr(VI), and As(V) on the aminated resin.

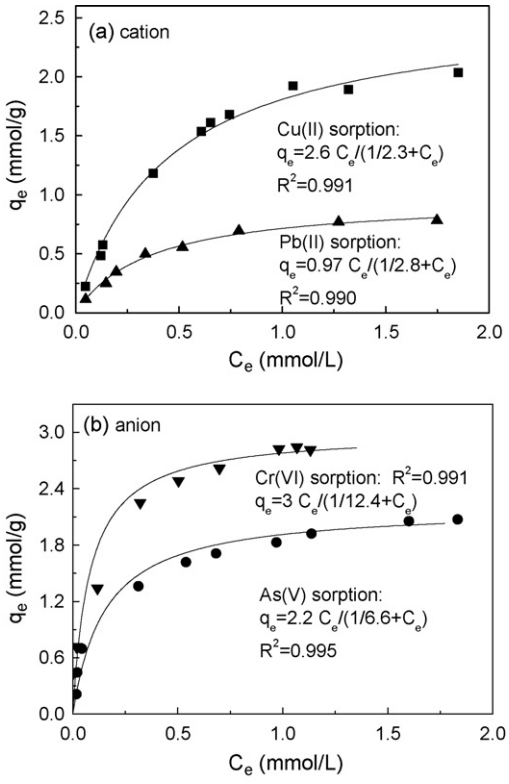

Fig. 6. Adsorption isotherms of Cu(II), Pb(II), Cr(VI), and As(V) on the aminated resin.

2.15 mmol/g, followed by Cr(VI), As(V), and Pb(II). The sorption process of adsorbates on porous adsorbents usually includes external diffusion, intraparticle diffusion, and adsorption on the active sites [27], where the intraparticle diffusion plays an important role in the sorption kinetics. In this study, the intraparticle diffusion may become slower since the long chain of polymer was grafted on the resin surface and intraparticle pore surfaces. At the same time, the sorption kinetics is also related to the sorption mechanism between the adsorbates and adsorbents, which will be discussed in the last section.

3.4. Sorption isotherm

Sorption isotherm has commonly been used to evaluate the adsorption capacity of an adsorbate on an adsorbent, and the Langmuir equation has been successfully used to model many sorption processes [25,28]. The Langmuir model assumes monolayer coverage of adsorbate over a homogeneous adsorbent surface, and the sorption of each molecule onto the surface has equal sorption activation energy. The Langmuir equation can be expressed as

$$q_e = \frac{q_m C_e}{1/b + C_e} \quad (1)$$

where q_m is the maximum sorption capacity (mmol/g), b is the sorption equilibrium constant (L/mmol), C_e is the equilibrium concentration of Cu(II), Pb(II), Cr(VI) or As(V) ions in solution (mmol/L).

Fig. 6 depicts the sorption isotherms of Cu(II), Pb(II), Cr(VI) and As(V) on the aminated resin. Their sorption capacities all increased with the increase of the equilibrium concentrations in solution. The Langmuir equation was used to fit the experimental data, and the corresponding parameters for the plot are given in Fig. 6. It can be seen that the Langmuir model described the experimental data well according to their high correlation coefficients (R^2), indicating that the monolayer sorption of the adsorbates possibly occurred on the resin. According to the Langmuir fitting, the maximum uptake capacity (q_m) is 2.6 mmol/g for Cu(II), 0.97 mmol/g for Pb(II), 3.0 mmol/g for Cr(VI), and 2.2 mmol/g for As(V). It was reported that when chitosan was grafted with polyacrylamide using ATRP, its maximum sorption capacity for mercury ions reached 322.6 mg/g, higher than 155 mg/g on the virgin chitosan bead [17]. The poly(acrylic acid)-grafted cross-linked poly(vinyl chloride) beads prepared by ATRP were used to remove some heavy metal ions such as Cu(II), Hg(II), Zn(II), and Cd(II) ions at pH 6, and their sorption capacities were in the range of 35–60 μmol/g [18]. Other researchers reported the cation exchange resin D001 had a maximum sorption capacity of 24 mg/g for Cu(II) at pH 5, while the maximum sorption capacity of Cu(II) on the polyethyleneimine-loaded resin D001-PEI was up to 99 mg/g (about 1.5 mmol/g) according to the Langmuir fitting [10]. The aminated resin modified by ethylenediamine had the sorption capacity of 1.73, 0.69 and 0.65 mmol/g for Hg(II), Cd(II) and Zn(II), respectively [29]. When the commercial resin IRA67 with polyamine group (5.6 mequiv./g) was used to remove Cu(II) under the same conditions as that in Fig. 1, the sorption capacity was only 0.43 mmol/g, perhaps due to the protonation of most amine groups. Obviously, the aminated resin prepared by ATRP in this study had satisfactory sorption capacities for the four adsorbates. The Langmuir constant (b) is 2.3 L/mmol for Cu(II) and 2.52 L/mmol for Pb(II), which are much lower than 12.4 L/mmol for Cr(VI) and 6.6 L/mmol for As(V), suggesting strong affinity of the aminated resin for anionic Cr(VI) and As(V) at pH 5.

3.5. Effect of solution pH

The effect of solution pH on the sorption of Cu(II), Pb(II), Cr(VI), and As(V) on the aminated resin is shown in Fig. 7. The adsorption of Cu(II) and Pb(II) on the resin was conducted at pH below 5.5 to avoid the formation of hydroxide precipitates. As shown in Fig. 7a, the sorption capacities of Cu(II) and Pb(II) increased with increasing solution pH. At pH below 2.2 for Cu(II) and 3.6 for Pb(II), almost no adsorption was observed, which was due to the protonated amine

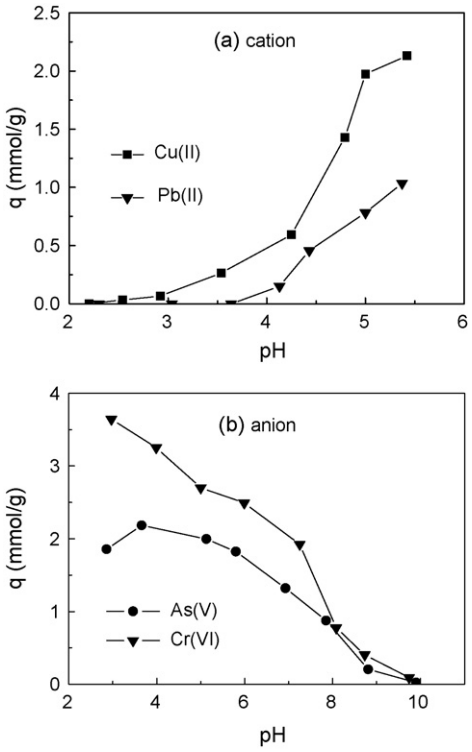

Fig. 7. Effect of pH on the adsorption of Cu(II), Pb(II), Cr(VI) and As(V) on the aminated resin (pH was kept constant by adding HCl or NaOH in the sorption process).

groups preventing the cationic adsorbates approaching the adsorption sites via electrostatic repulsion. With the increase of solution pH, some amine groups on the resin may chelate Cu(II) and Pb(II). The low sorption capacity at low pH indicates that the spent resin can be regenearated in acidic solution. After 0.05 g resin was placed into 100 mL of 2 mM Cu(II) or Pb(II) solution at pH 5 for 12 h, the spent resin was filtered and put into 100 mL of 0.1 M HCl solution for 4 h, their regeneration rates were all above 99%, suggesting that the aminated resin can be regenerated and reused for the removal of cationic heavy metals.

Fig. 7b illustrates the pH effect on the anionic Cr(VI) and As(V) sorption on the resin. The sorption capacity of Cr(VI) decreased with increasing solution pH in the pH range studied, and the adsorption capacity decreased from 3.6 mmol/g at pH 3 to 0.1 mmol/g at pH 9.7. In contrast, the sorption capacity of As(V) first increased and then decreased at pH above 3.7, and almost no adsorption was observed at pH 9.9. Since more As(V) are present as H_3AsO_4 at pH 2.9 [30], and it cannot be adsorbed on the protonated amine groups via electrostatic interaction, the sorption capacity is lower at pH 2.9 than that at pH 3.7. Since As(V) exists as $H_2AsO_4^-$, $HAsO_4^{2-}$, and AsO_4^{3-} species in aqueous solution at pH from 4 to 10 [30], electrostatic attraction should play an important role in the sorption of anionic arsenic on the protonated amine resin. With the increase of solution pH, the number of protonated amine groups decreased, resulting in the decrease of sorption capacity of As(V). Similarly, Cr(VI) is present as anions ($HCrO_4^-$, CrO_4^{2-} and $Cr_2O_7^{2-}$) at pH above 3 [31], electrostatic interaction should dominate the sorption. Actually, the different sorption behaviors of cationic and anionic adsorbates on the aminated resin indicate the different sorption mechanism in the adsorption process, which will be further discussed in the next section. In addition, when the spent resin after As(V) and Cr(VI) sorption was placed into 100 mL of 0.1 M NaOH solution, the desorption rate was 86% for As(V), and only 39% for Cr(VI). The different desorption rates indicate the complicated adsorption for anionic adsorbates.

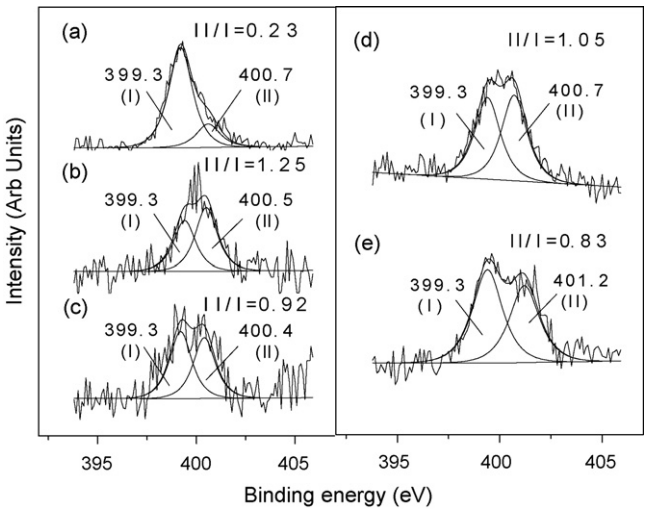

Fig. 8. XPS N 1s core-level spectra of (a) aminated resin before sorption, (b) Cu-adsorbed, (c) Pb-adsorbed resin, (d) Cr-adsorbed, and (e) As-adsorbed resin.

3.6. Sorption mechanism

XPS has often been used to identify the interaction of an adsorbate with the surface functional groups on an adsorbent because the creation of a chemical bond between them changes the distribution of the electrons around the corresponding atoms [2,32]. The N 1s core-level XPS spectra of the aminated resin before and after Cu(II), Pb(II), Cr(VI) and As(V) sorption were examined. Fig. 8a presents the spectrum of the aminated resin before sorption, and the BEs at 399.3 and 400.7 eV are attributed to the nitrogen in the $-NH_2$ ($-NH-$) and $-NH_3^+$ ($-NH_2^+-$), respectively [25]. About 19% amine groups were protonated before adsorption. After cationic Cu(II) and Pb(II) were adsorbed on the resin at pH 5, the peaks at higher BEs of 400.5 and 400.4 eV were obtained, and their area ratios increased significantly, indicating that Cu(II) and Pb(II) ions were adsorbed on the amine groups on the resin. The lone pair of electrons in the nitrogen atoms of the amine group can be donated to form a shared bond between Cu(II) or Pb(II) and the nitrogen atoms, resulting in the higher BEs observed. The adsorption of Cu(II) and Pb(II) ions on the amine groups ($-NH-$ and $-NH_2$) via chelation interaction on the resin can be expressed as follows (using $-NH_2$ and Cu(II) as representatives):

$$-NH_2 + Cu^{2+} \rightarrow -NH_2-Cu^{2+} \text{ or } -NH_2-Cu^{2+}-NH_2- \quad (2)$$

Since some amine groups can be protonated at pH 5, they cannot adsorb Cu(II) or Pb(II) ions via chelation. Therefore, the peaks at 400.5 and 400.4 eV in Fig. 8b and c should be the combination of the nitrogen in the protonated amine groups and deprotonated amine groups chelating Cu(II) or Pb(II) ions.

Fig. 8d and e show the N 1s spectra of the aminated resin after the anionic Cr(VI) and As(V) sorption, and the higher BEs peaks at 400.7 and 401.2 eV are attributed to the protonated nitrogen atom on the resin. The proportion of the positively charged nitrogen atoms (peak II) to the uncharged nitrogen atoms (peak I) on the resin surface significantly increased after Cr(VI) and As(V) sorption compared to that in Fig. 8a, suggesting that the protonated amine groups are responsible for Cr(VI) and As(V) sorption. The amine groups were first protonated at pH 5, and then adsorbed the negative Cr(VI) and As(V) ions. The protonated amine groups adsorbed anionic As(V) ($H_2AsO_4^-$) at pH 5 via electrostatic attraction as follows (using $-NH_2$ and $H_2AsO_4^-$ as representatives):

$$-NH_3^+ + H_2AsO_4^- \rightarrow -NH_3^+ \ldots H_2AsO_4^- \quad (3)$$

Similarly, $HCrO_4^-$ is the major species (about 86%) at pH 5 in this study [33], and it can be adsorbed on the protonated amine groups on the resin as follows:

$$-NH_3^+ + HCrO_4^- \rightarrow -NH_3^+ \ldots HCrO_4^- \quad (4)$$

4. Conclusions

A novel aminated resin was successfully prepared via SI-ATRP and amination reactions. The optimal ATRP time was found to be 100 min, while 10 h was required in the amination reaction to achieve the best aminated resin with high sorption capacity for Cu(II). Some grafted polymer brushes were observed on the resin surface using SEM. The amine groups introduced on the resin surface and intraparticle pores provided more adsorption sites for both cationic and anionic adsorbates. Sorption isotherms show that the adsorption capacities of Cu(II), Pb(II), Cr(VI), and As(V) on the aminated resin at pH 5 were 2.6, 0.97, 3.0, and 2.2 mmol/g, respectively. Solution pH had significant effect on their sorption, and the adsorption capacities of Cu(II) and Pb(II) increased with increasing solution pH, while the sorption capacities of Cr(VI) and As(V) decreased with increasing pH. XPS spectra proved that chelation interaction between the amine groups on the resin and cationic heavy metals occurred, while the electrostatic interaction played an important role in the adsorption of anionic Cr(VI) and As(V). This study shows that the aminated resin prepared by SI-ATRP had high sorption capacities for both cationic and anionic pollutants, implying a promising application in heavy metal removal from wastewater.

Acknowledgments

This research was supported by Program for New Century Excellent Talents in University and National Outstanding Youth Foundation of China (50625823). The analytical work was supported by the Laboratory Fund of Tsinghua University.

References

[1] M.V. Dinu, E.S. Dragan, Evaluation of Cu^{2+}, Co^{2+} and Ni^{2+} ions removal from aqueous solution using a novel chitosan/clinoptilolite composite: kinetics and isotherms, Chem. Eng. J. 160 (2010) 157–163.
[2] S.B. Deng, R.B. Bai, J.P. Chen, Aminated polyacrylonitrile fibers for lead and copper removal, Langmuir 19 (2003) 5058–5064.
[3] S. Schiewer, M. Iqbal, The role of pectin in Cd binding by orange peel biosorbents: a comparison of peels, depectinated peels and pectic acid, J. Hazard. Mater. 177 (2010) 899–907.
[4] C.H. Xiong, C.P. Yao, Synthesis, characterization and application of triethylenetetramine modified polystyrene resin in removal of mercury, cadmium and lead from aqueous solutions, Chem. Eng. J. 155 (2009) 844–850.
[5] Y.H. Xu, D.Y. Zhao, Removal of copper from contaminated soil by use of poly(amidoamine) dendrimers, Environ. Sci. Technol. 39 (2005) 2369–2375.
[6] C.O. Ijagbemi, M.H. Baek, D.S. Kim, Montmorillonite surface properties and sorption characteristics for heavy metal removal from aqueous solutions, J. Hazard. Mater. 166 (2009) 538–546.
[7] A. Benhamou, M. Baudu, Z. Derriche, J.P. Basly, Aqueous heavy metals removal on amine-functionalized Si-MCM-41 and Si-MCM-48, J. Hazard. Mater. 171 (2009) 1001–1008.
[8] Z.K. Yang, Y. Yuan, Y.T. Wang, Synthesis and evaluation of chitosan aryl azacrown ethers as adsorbents for metal ions, J. Appl. Polym. Sci. 77 (2000) 3093–3098.
[9] S.B. Deng, R. Ma, Q. Yu, J. Huang, G. Yu, Enhanced removal of pentachlorophenol and 2,4-D from aqueous solution by an aminated biosorbent, J. Hazard. Mater. 165 (2009) 408–414.
[10] Y.L. Chen, B.C. Pan, H.Y. Li, W.M. Zhang, L. Lv, J. Wu, Selective removal of Cu(II) ions by using cation-exchange resin-supported polyethyleneimine (PEI) nanoclusters, Environ. Sci. Technol. 44 (2010) 3508–3513.
[11] S. Cavus, G. Gurdag, K. Sozgen, M.A. Gurkaynak, The preparation and characterization of poly(acrylic acid-co-methacrylamide) gel and its use in the non-competitive heavy metal removal, Polym. Adv. Technol. 20 (2009) 165–172.
[12] J.S. Wang, K. Matyjaszewski, Controlled living radical polymerization atom-transfer radical polymerization in the presence of transition-metal complexes, J. Am. Chem. Soc. 117 (1995) 5614–5615.
[13] F.J. Xu, K.G. Neoh, E.T. Kang, Bioactive surfaces and biomaterials via atom transfer radical polymerization, Prog. Polym. Sci. 34 (2009) 719–761.
[14] S. Edmondson, V.L. Osborne, W.T.S. Huck, Polymer brushes via surface-initiated polymerizations, Chem. Soc. Rev. 33 (2004) 14–22.
[15] V. Stadler, R. Kirmse, M. Beyer, F. Breitling, T. Ludwig, F.R. Bischoff, PEGMA/MMA copolymer graftings: generation, protein resistance, and a hydrophobic domain, Langmuir 24 (2008) 8151–8157.
[16] F.J. Xu, E.T. Kang, K.G. Neoh, LTV-induced coupling of 4-vinylbenzyl chloride on hydrogen-terminated Si(1 0 0) surfaces for the preparation of well-defined polymer-Si hybrids via surface-initiated ATRP, Macromolecules 38 (2005) 1573–1580.
[17] N. Li, R.B. Bai, C.K. Liu, Enhanced and selective adsorption of mercury ions on chitosan beads grafted with polyacrylamide via surface-initiated atom transfer radical polymerization, Langmuir 21 (2005) 11780–11787.
[18] P. Liu, Y.S. Liu, Z.X. Su, Modification of poly(hydroethyl acrylate)-grafted cross-linked poly(vinyl chloride) particles via surface-initiated atom-transfer radical polymerization (SI-ATRP): competitive adsorption of some heavy metal ions on modified polymers, Ind. Eng. Chem. Res. 45 (2006) 2255–2260.
[19] B.F. Senkal, E. Yavuz, Preparation of poly(vinyl pyrrolidone) grafted sulfonamide based polystyrene resin and its use for the removal of dye from water, Polym. Adv. Technol. 17 (2006) 928–931.
[20] E. Yavuz, G. Bayramoglu, B.F. Senkal, M.Y. Arica, Poly(glycidylmethacrylate) brushes generated on poly(VBC) beads by SI-ATRP technique: hydrazine and amino groups functionalized for invertase adsorption and purification, J. Chromatogr. B 877 (2009) 1479–1486.
[21] F.J. Xu, J.P. Zhao, E.T. Kang, K.G. Neoh, J. Li, Functionalization of nylon membranes via surface-initiated atom-transfer radical polymerization, Langmuir 23 (2007) 8585–8592.
[22] F.J. Xu, Q.J. Cai, E.T. Kang, K.G. Neoh, Surface-initiated atom transfer radical polymerization from halogen-terminated Si(1 1 1) (Si-X, X = Cl, Br) surfaces for the preparation of well-defined polymer-Si hybrids, Langmuir 21 (2005) 3221–3225.
[23] G. Bayramoglu, E. Yavuz, B.F. Senkal, M.Y. Arica, Glycidyl methacrylate grafted on p(VBC) beads by SI-ATRP technique: Modified with hydrazine as a salt resistance ligand for adsorption of invertase, Colloid Surface A 345 (2009) 127–134.
[24] R.L. Shriner, C.K.F. Hermann, T.C. Morrill, D.Y. Curtin, R.C. Fuson, The Systematic Identification of Organic Compounds, eighth ed., John Wiley & Sons, New York, 2004.
[25] S.B. Deng, G. Yu, S.H. Xie, Q. Yu, J. Huang, Y. Kuwaki, M. Iseki, Enhanced adsorption of arsenate on the aminated fibers: sorption behavior and uptake mechanism, Langmuir 24 (2008) 10961–10967.
[26] F.J. Xu, Z.H. Wang, W.T. Yang, Surface functionalization of polycaprolactone films via surface-initiated atom transfer radical polymerization for covalently coupling cell-adhesive biomolecules, Biomaterials 31 (2010) 3139–3147.
[27] N.K. Lazaridis, D.D. Asouhidou, Kinetics of sorptive removal of chromium(VI) from aqueous solutions by calcined Mg–Al–CO_3 hydrotalcite, Water Res. 37 (2003) 2875–2882.
[28] S.B. Deng, Y.P. Ting, Fungal biomass with grafted poly(acrylic acid) for enhancement of Cu(II) and Cd(II) biosorption, Langmuir 21 (2005) 5940–5948.
[29] A.A. Atia, A.M. Donia, A.M. Yousif, Synthesis of amine and thio chelating resins and study of their interaction with zinc(II), cadmium(II) and mercury(II) ions in their aqueous solutions, React. Funct. Polym. 56 (2003) 75–82.
[30] Z.J. Li, S.B. Deng, G. Yu, J. Huang, V.C. Lim, As(V) and As(III) removal from water by a Ce–Ti oxide adsorbent: behavior and mechanism, Chem. Eng. J. 161 (2010) 106–113.
[31] S.B. Deng, Y.P. Ting, Polyethylenimine-modified fungal biomass as a high-capacity biosorbent for Cr(VI) anions: sorption capacity and uptake mechanisms, Environ. Sci. Technol. 39 (2005) 8490–8496.
[32] R.B. Bai, X. Zhang, Polypyrrole-coated granules for humic acid removal, J. Colloid Interf. Sci. 243 (2001) 52–60.
[33] L.K. Cabatingan, R.C. Agapay, J.L.L. Rakels, M. Ottens, L.A.M. van der Wielen, Potential of biosorption for the recovery of chromate in industrial wastewaters, Ind. Eng. Chem. Res. 40 (2001) 2302–2309.